Stanford Exploration Project, Report 79, November 16, 1997, pages 1–241

Angle-dependent reflectivity estimation by Kirchhoff migration/inversion: Theory

David E. Lumley and Wafik B. Beydoun[1 2]

keywords: *reflectivity, modeling, approximation, elastic, diffraction, estimation, divergence, least squares, phase, prestack*

ABSTRACT

We derive a new Kirchhoff forward and inverse theory for modeling and estimating P-P angle-dependent reflectivity. We replace conventional reflecting surface excitations by *equivalent body force* volumetric excitations, and then linearize the divergence of the elastic stress tensor wavefield with respect to smooth background material properties. To obtain the reflected wavefield, we perform a volume integral over the equivalent body force distribution, and interpret this result as a hybrid of Zoeppritz plane-wave reflection and Rayleigh-Sommerfeld elastic diffraction. We pose the inverse problem as a least-squares optimization to estimate angle-dependent reflectivity, including the reflection angles, by minimizing the squared error between the forward theory predictions and the observed seismograms. The resulting coupled normal equations are decoupled by the method of stationary phase, and then the uncoupled equations are solved by a classical Gauss-Newton gradient method with an approximate diagonal Hessian operator. The estimation for angle-dependent reflectivity requires a simultaneous calculation of four differently weighted Kirchhoff prestack depth migrations, which combine to compensate for limited acquisition aperture and enhanced reflection amplitude recovery.

INTRODUCTION

Estimation of angle-dependent reflectivity is a critical step in the larger inverse problem of mapping subsurface material properties from surface seismic reflection data (e.g., Lumley and Beydoun, 1991). The latter is, in turn, important for hydrocarbon exploration and detection, and crucial for reservoir characterization and monitoring in the development and production phases.

[2]**email:** not available

[2]Elf Geoscience Research Centre, London, UK.

Stolt and Weglein (1985) gave a comprehensive review of linearized seismic migration and inversion techniques, which we recommend as useful background information to the angle-dependent reflectivity analysis we present here. Bleistein (1987) addressed the angle-dependent reflectivity problem based on the work of Beylkin (1985). By a suitable choice of a Kirchhoff integrand, Bleistein was able to show that his trial solution reduced to an estimate of angle-dependent reflectivity under the stationary phase approximation. However, it is not clear that the solution is robust in the sense of an l_p-norm estimate, nor that it can be derived in a straightforward inverse theory approach, starting with an explicit forward model for reflection and diffraction.

More recently, de Bruin (1992) and Cunha (1992) approached this problem from a finite-difference perspective. de Bruin estimates angle-dependent reflectivity using an ω-x migration scheme. However, de Bruin processes the data in constant ray parameter sections, and so cannot estimate the reflection angles directly from the data, without a posteriori information on the geologic structure and dip. His suggestion of a second-pass procedure of evaluating the reflection angles after picking migrated reflector horizons may represent an inefficient and unstable process. Cunha (1992) applied a reverse-time migration procedure to estimate angle-dependent reflectivity. As with de Bruin, Cunha needs to invoke and evaluate a set of new imaging conditions to estimate reflectivity, but, unlike de Bruin, Cunha is able to directly estimate reflection angles from the data. Possible disadvantages to Cunha's method are its prohibitive computational expense, and its potential for instability due to its formulation in the common-shot domain.

In this paper we derive a robust least-squares estimate of angle-dependent reflectivity. We start from an elastic representation theorem-based forward modeling theory of generalized diffraction and reflection, and invoke a straightforward application of least-squares inverse theory. The method does not require the arbitrary definition of any particular imaging conditions, and both reflectivity and reflection angle are directly estimated from the data without a priori knowledge of structural dip. The results can be interpreted as a least-squares generalization of Bleistein's approach, and cost little more than a standard Kirchhoff prestack migration to implement.

This paper proceeds as follows. We first derive a forward theory relating angle-dependent seismic reflection data to a generalized reflection model which combines elements of Zoeppritz plane-wave reflection and Rayleigh-Sommerfeld elastic diffraction. On the basis of this forward model, we formulate a least-squares inverse problem to estimate the angle-dependent reflection coefficient as a function of subsurface coordinate and offset. This analysis leads to two coupled normal equations for reflectivity and reflection angle, as a function of the recorded seismic data. We decouple the two equations using a stationary phase approximation. We finally solve the reflectivity and angle equations separately using a standard Gauss-Newton gradient optimization technique and an approximate diagonal Hessian operator.

FORWARD MODELING THEORY

Reflectivity representation theorems

Consider the elastodynamic wave equation for a displacement vector field $\mathbf{u}_1$ and second order stress tensor field σ_1 due to a body force vector excitation $\mathbf{f}_1$:

$$-\rho\omega^2 \mathbf{u}_1 = \nabla\cdot\sigma_1 + \mathbf{f}_1 \ , \tag{1}$$

as per Aki and Richards (1980, p.19, eqn. 2.17). Consider a second displacement and stress field $\mathbf{u}_2$ and σ_2, with body force $\mathbf{f}_2$, which also satisfy the elastodynamic wave equation:

$$-\rho\omega^2 \mathbf{u}_2 = \nabla\cdot\sigma_2 + \mathbf{f}_2 \ . \tag{2}$$

The two sets of elastic wavefield can be related by the Divergence Theorem:

$$\int_{\mathcal{V}} \nabla\cdot(\sigma_1\cdot\mathbf{u}_2 - \sigma_2\cdot\mathbf{u}_1)\, d\mathcal{V} = \int_{\mathcal{S}} \hat{\mathbf{n}}\cdot(\sigma_1\cdot\mathbf{u}_2 - \sigma_2\cdot\mathbf{u}_1)\, d\mathcal{S} \ . \tag{3}$$

We assume that the scattered (reflected + diffracted) wavefield within the volume $\mathcal{V}$ is due to a volumetric body force equivalent of reflection surface excitations. This means that, although reflections are created by reflector surface discontinuities in material properties as shown later, we represent those surface excitations as *equivalent volumetric body forces*, as opposed to conventional surface tractions. In this case, we can write the forward theory explicitly as a mapping from interior points $\mathbf{x}$ in the volume $\mathcal{V}$ to an recording surface $\mathcal{S}$. More importantly, the inverse theory is an explicit map from the recorded surface data on $\mathcal{S}$ to the equivalent body force functions at all $\mathbf{x}$ within $\mathcal{V}$, rather than to arbitrary reflection surfaces $\mathcal{S}'$ within $\mathcal{V}$. This distinction is subtle yet critical for a rigorous solution to the angle-dependent reflectivity inverse problem.

Under the body force equivalence assumption, the surface integral in (3) vanishes (no volume boundary effects):

$$\int_{\mathcal{V}} \nabla\cdot(\sigma_1\cdot\mathbf{u}_2 - \sigma_2\cdot\mathbf{u}_1)\, d\mathcal{V} = 0 \ . \tag{4}$$

For any vector $\mathbf{u}$ and second order tensor σ,

$$\nabla\cdot(\sigma\cdot\mathbf{u}) = (\nabla\cdot\sigma)\cdot\mathbf{u} + \sigma{:}\nabla\mathbf{u} \ , \tag{5}$$

where $\sigma{:}\nabla\mathbf{u}$ is a second-order inner contraction of σ with $\nabla\mathbf{u}$, and is equivalent to their dot product in this specific case. Using identity (5), (4) can be expanded as:

$$\int_{\mathcal{V}} [(\nabla\cdot\sigma_1)\cdot\mathbf{u}_2 - (\nabla\cdot\sigma_2)\cdot\mathbf{u}_1 + \sigma_1{:}\nabla\mathbf{u}_2 - \sigma_2{:}\nabla\mathbf{u}_1] \, d\mathcal{V} = 0 \; . \tag{6}$$

We next assume a linear elastic stress-strain relationship such that

$$\sigma = \mathbf{C}{:}\nabla\mathbf{u} \; , \tag{7}$$

where $\mathbf{C}$ is the fourth-order elastic stiffness tensor C_{ijkl}. Due to the symmetries inherent in $\mathbf{C}$ (Aki and Richards, 1980, p.20),

$$\sigma_1\cdot\nabla\mathbf{u}_2 = (\mathbf{C}{:}\nabla\mathbf{u}_1){:}\nabla\mathbf{u}_2 = \nabla\mathbf{u}_1{:}\mathbf{C}{:}\nabla\mathbf{u}_2 = \nabla\mathbf{u}_2{:}\mathbf{C}{:}\nabla\mathbf{u}_1 = \sigma_2{:}\nabla\mathbf{u}_1 \; , \tag{8}$$

after Frazer and Sen (1985, p.123), for example.

Thus, $(\sigma_1{:}\nabla\mathbf{u}_2 - \sigma_2{:}\nabla\mathbf{u}_1) = 0$ and so (6) becomes:

$$\int_{\mathcal{V}} [(\nabla\cdot\sigma_1)\cdot\mathbf{u}_2 - (\nabla\cdot\sigma_2)\cdot\mathbf{u}_1] \, d\mathcal{V} = 0 \; . \tag{9}$$

The difference between the two dot-product equations $\mathbf{u}_2\cdot$eqn(1) and $\mathbf{u}_1\cdot$eqn(2) can be written as

$$\mathbf{u}_2\cdot(\nabla\cdot\sigma_1) - \mathbf{u}_1\cdot(\nabla\cdot\sigma_2) = \mathbf{f}_2\cdot\mathbf{u}_1 - \mathbf{f}_1\cdot\mathbf{u}_2 \; . \tag{10}$$

Substituting (10) into (9) yields

$$\int_{\mathcal{V}} (\mathbf{f}_2\cdot\mathbf{u}_1 - \mathbf{f}_1\cdot\mathbf{u}_2) \, d\mathcal{V} = 0 \; , \tag{11}$$

as per Aki and Richards (1980, p.27, eqn. 2.35) with the surface integral terms set to zero. We specify $\mathbf{f}_2$ such that

$$\mathbf{f}_2 = \hat{\mathbf{a}}_r \delta(\mathbf{x} - \mathbf{x}_r) \; , \tag{12}$$

where $\hat{\mathbf{a}}_r$ selects an arbitrary component of the vector wavefield $\mathbf{u}_2$ at the receiver location $\mathbf{x}_r$. The delta function form (12) of $\mathbf{f}_2$ implies that $\mathbf{u}_2$ is by definition a solution to the Green's function problem:

$$\rho\omega^2\mathbf{u}_2 + \nabla\cdot\sigma_2 = -\hat{\mathbf{a}}_r \delta(\mathbf{x} - \mathbf{x}_r) \; , \tag{13}$$

such that

$$\mathbf{u}_2(\mathbf{x};\mathbf{x}_r) = \hat{\mathbf{a}}_r\cdot\mathbf{G}(\mathbf{x};\mathbf{x}_r) \; , \tag{14}$$

where $\mathbf{G}$ is the second order Green's tensor. In this case, substituting (12) into (11) and integrating out the delta function reveals:

$$\hat{\mathbf{a}}_r \cdot \mathbf{u}_1(\mathbf{x}_r) = \int_{\mathcal{V}} \mathbf{f}_1(\mathbf{x}) \cdot \mathbf{u}_2(\mathbf{x}; \mathbf{x}_r)\, d\mathcal{V} \ . \tag{15}$$

Equation (15) is our volume integral representation of the reflected wavefield $\mathbf{u}_1$ at $\mathbf{x}_r$, due to a body force equivalent $\mathbf{f}_1$ of reflective surface excitation, weighted against the source wavefield $\mathbf{u}_2$ at each subsurface point $\mathbf{x}$.

Generalized scattering

To proceed, we use isotropic elastic WKBJ (ray-valid) Green's tensors for P waves of the form:

$$\mathbf{u}^{P}(\mathbf{x}; \mathbf{x}') = A^{P}(\mathbf{x}; \mathbf{x}')\ \hat{\mathbf{t}}^{P}(\mathbf{x}; \mathbf{x}')\ e^{i\omega\tau(\mathbf{x};\mathbf{x}')} = A^{P} \hat{\mathbf{t}}^{P} e^{i\omega\tau} \ , \tag{16}$$

where A^{P} and τ are the ray-valid P-wave amplitude and traveltime from the "source" location $\mathbf{x}'$ to the "observation" point $\mathbf{x}$. The unit vector $\hat{\mathbf{t}}^{P}$ is the direction parallel to P-wave propagation, and is perpendicular to the wavefronts τ = constant. Given the definition of $\mathbf{u}^{P}$ in (16), we derive the following useful quantities:

$$|\mathbf{u}^{P}| = \mathbf{u}^{P} \cdot \hat{\mathbf{t}}^{P} = A^{P} e^{i\omega\tau} \ , \tag{17}$$

$$\nabla \cdot \mathbf{u}^{P} = i\omega \nabla\tau \cdot \mathbf{u}^{P} = \frac{i\omega}{\alpha} \hat{\mathbf{t}}^{P} \cdot \mathbf{u}^{P} = \frac{i\omega}{\alpha} A^{P} e^{i\omega\tau} = \frac{i\omega}{\alpha} |\mathbf{u}^{P}| \ , \tag{18}$$

and

$$\nabla \mathbf{u}^{P} = i\omega \nabla\tau \mathbf{u}^{P} + \mathrm{O}(\nabla A^{P}) \approx \frac{i\omega}{\alpha} \hat{\mathbf{t}}^{P} \mathbf{u}^{P} \ , \tag{19}$$

where $\alpha(\mathbf{x})$ is the compressional wave velocity. In the gradient equation (19) for $\nabla \mathbf{u}^{P}$ we have used the fact that

$$\nabla\tau = \frac{1}{\alpha} \hat{\mathbf{t}}^{P} \ , \tag{20}$$

which follows from the ray eikonal equation defining the traveltime τ:

$$|\nabla\tau|^2 = \nabla\tau \cdot \nabla\tau = \frac{1}{\alpha^2} \ , \tag{21}$$

(Červený et al., 1977), and the farfield approximation that

$$\frac{|\nabla A^{P}|}{|A^{P}|} \ll 1 \; , \tag{22}$$

since $A \sim 1/r$ and so $|\nabla A| \sim 1/r^2$.

Now, we choose $\mathbf{u}_1 \equiv \mathbf{u}^{P}(\mathbf{x};\mathbf{x}_s)$ to get the P-wave reflectivity response at the subsurface point $\mathbf{x}$ from the source location $\mathbf{x}_s$. Under the previous assumption of linear elastic isotropy for $\mathbf{u}^{P}$, the stress-strain relationship is isotropic such that

$$\sigma^{P} = \left[\lambda(\nabla\cdot\mathbf{u}^{P})\mathbf{I} + 2\mu\nabla\mathbf{u}^{P}\right] = \frac{i\omega}{\alpha}\left[\lambda(\hat{\mathbf{t}}^{P}\cdot\mathbf{u}^{P})\mathbf{I} + 2\mu\hat{\mathbf{t}}^{P}\mathbf{u}^{P}\right] \; , \tag{23}$$

where $\lambda(\mathbf{x})$ and $\mu(\mathbf{x})$ are the Lamé parameters, and $\mathbf{I}$ is the second-order identity matrix δ_{ij}. The expression for the divergence of the stress field becomes

$$\nabla\cdot\sigma^{P} = \text{term } 1 + \text{term } 2 \; , \tag{24}$$

where

$$\text{term } 1 = \frac{i\omega}{\alpha}\left[\lambda\nabla(\hat{\mathbf{t}}^{P}\cdot\mathbf{u}^{P}) + 2\mu\nabla\cdot(\hat{\mathbf{t}}^{P}\mathbf{u}^{P})\right] \; , \tag{25}$$

and

$$\text{term } 2 = \frac{i\omega}{\alpha^2}\left[(\alpha\nabla\lambda - \lambda\nabla\alpha)(\hat{\mathbf{t}}^{P}\cdot\mathbf{u}^{P}) + 2(\alpha\nabla\mu - \mu\nabla\alpha)\cdot(\hat{\mathbf{t}}^{P}\mathbf{u}^{P})\right] \; , \tag{26}$$

where we have used the identities:

$$\nabla\cdot(\alpha\mathbf{I}) = \nabla\alpha \; , \tag{27}$$

and

$$\nabla\cdot(\alpha\sigma) = \alpha\nabla\cdot\sigma + \nabla\alpha\cdot\sigma \; , \tag{28}$$

for any scalar α and second order tensor σ (Ben-Menahem and Singh, 1981, p.953). Now, using the identity

$$\nabla\cdot(\mathbf{u}\mathbf{v}) = (\nabla\cdot\mathbf{u})\mathbf{v} + \mathbf{u}\cdot\nabla\mathbf{v} \; , \tag{29}$$

for any two vectors $\mathbf{u}$ and $\mathbf{v}$, and the fact that

$$\nabla\cdot\hat{\mathbf{t}}^{P} = 0 \, , \tag{30}$$

we rewrite (25) as

$$\begin{aligned} \text{term 1} &= \frac{i\omega}{\alpha}\left[\lambda(\hat{\mathbf{t}}^{P}\cdot\nabla\mathbf{u}^{P}) + 2\mu(\hat{\mathbf{t}}^{P}\cdot\nabla\mathbf{u}^{P})\right] \\ &= \frac{i\omega}{\alpha}(\lambda+2\mu)(\hat{\mathbf{t}}^{P}\cdot\nabla\mathbf{u}^{P}) \\ &= \frac{i\omega}{\alpha}(\lambda+2\mu)\frac{i\omega}{\alpha}\mathbf{u}^{P} \\ &= -\rho\omega^2\mathbf{u}^{P} \, , \end{aligned} \tag{31}$$

where we have used (18) and the definition:

$$\lambda + 2\mu = \rho\alpha^2 \, . \tag{32}$$

Furthermore, we compress the dot products in (26) to yield:

$$\text{term 2} = \frac{i\omega}{\alpha^2}|\mathbf{u}^{P}|\left[(\alpha\nabla\lambda - \lambda\nabla\alpha) + 2(\alpha\nabla\mu - \mu\nabla\alpha)\cdot(\hat{\mathbf{t}}^{P}\hat{\mathbf{t}}^{P})\right] \, , \tag{33}$$

Recalling the elastic wave equation

$$\mathbf{f}^{P} = -\rho\omega^2\mathbf{u}^{P} - \nabla\cdot\sigma^{P} \tag{34}$$

and substituting (31) and (33) for the stress divergence term, we arrive at the following expression for the body force $\mathbf{f}^{P}$:

$$\mathbf{f}^{P} = -\frac{i\omega}{\alpha^2}|\mathbf{u}^{P}|\left[(\alpha\nabla\lambda - \lambda\nabla\alpha) + 2(\alpha\nabla\mu - \mu\nabla\alpha)\cdot(\hat{\mathbf{t}}^{P}\hat{\mathbf{t}}^{P})\right] \, . \tag{35}$$

Equation (35) is a *body force equivalent* for surface reflectivity excitations, and is clearly dependent on material property contrasts (gradients): $\nabla\alpha$, $\nabla\lambda$ and $\nabla\mu$.

At this point, it is convenient to make an analogy to Born elastic scattering (Beydoun and Mendes, 1989) in that we can write

$$\nabla\cdot\sigma^{P} = \nabla_o\cdot\sigma^{P} + \nabla\cdot\sigma^{\delta m} \, , \tag{36}$$

where ∇_o is the gradient with respect to a reflectionless *smooth background* model, and $\nabla\cdot\sigma^{\delta m}$ is the stress divergence field associated with the true model material property contrasts: $\nabla\alpha$, $\nabla\lambda$ and $\nabla\mu$, which give rise to the scattered wavefield. The two stress divergence terms can be associated with (31) and (33) such that:

$$\text{term 1} = \nabla_o \cdot \sigma^{P} = -\rho\omega^2 \mathbf{u}^{P} \,, \tag{37}$$

which is the background wavefield, and

$$\text{term 2} = \nabla \cdot \sigma^{\delta m} = -\frac{i\omega}{\alpha^2} |\mathbf{u}^{P}| \left[(\alpha\nabla\lambda - \lambda\nabla\alpha) + 2(\alpha\nabla\mu - \mu\nabla\alpha) \cdot (\hat{\mathbf{t}}^{P} \hat{\mathbf{t}}^{P}) \right] \,, \tag{38}$$

which is the scattered wavefield.

To obtain the reflected field at the receiver position $\mathbf{x}_r$, recall the volume integral representation (15) for P waves:

$$\hat{\mathbf{a}}_r \cdot \mathbf{u}^{P}(\mathbf{x}_r, \mathbf{x}_s) = \int_{\mathcal{V}} \mathbf{f}^{P}(\mathbf{x}; \mathbf{x}_s) \cdot \mathbf{u}_2(\mathbf{x}; \mathbf{x}_r) \, d\mathcal{V}(\mathbf{x}) \,. \tag{39}$$

We substitute the WKBJ Green's tensor for the wavefield $\mathbf{u}^{P}$ and $\mathbf{u}_2$ as defined by (16) and (14):

$$\mathbf{u}^{P}(\mathbf{x}; \mathbf{x}_s) = A^{P}(\mathbf{x}; \mathbf{x}_s) e^{i\omega\tau(\mathbf{x};\mathbf{x}_s)} \hat{\mathbf{t}}^{P}(\mathbf{x}; \mathbf{x}_s) \rightarrow A_s e^{i\omega\tau_s} \hat{\mathbf{t}}_s^{P} \,, \tag{40}$$

and

$$\mathbf{u}_2(\mathbf{x}; \mathbf{x}_r) = A^{P}(\mathbf{x}; \mathbf{x}_r) e^{i\omega\tau(\mathbf{x};\mathbf{x}_r)} \hat{\mathbf{t}}^{P}(\mathbf{x}; \mathbf{x}_r) [\hat{\mathbf{a}}_r(\mathbf{x}_r) \cdot \hat{\mathbf{t}}^{P}(\mathbf{x}_r)] \rightarrow A_r e^{i\omega\tau_r} \hat{\mathbf{t}}_r^{P} \,, \tag{41}$$

where

$$A_r = A^{P}(\mathbf{x}; \mathbf{x}_r) \cos \hat{\mathbf{a}}_r(\mathbf{x}_r) \,, \tag{42}$$

and

$$\cos a_r(\mathbf{x}_r) = [\hat{\mathbf{a}}_r(\mathbf{x}_r) \cdot \hat{\mathbf{t}}^{P}(\mathbf{x}_r)] \,. \tag{43}$$

The latter is evaluated at $\mathbf{x}_r$, and all other compact quantities are evaluated at $\mathbf{x}$. The factor $\cos a_r$ is required for multi-component displacement data. For example, if 3-component data are available, or if pressure data are recorded (marine), then $\cos a_r = 1$ and $\hat{\mathbf{a}}_r \cdot \mathbf{u}^{P} = |\mathbf{u}^{P}|$. Or, if only vertical component data are available, then $\cos a_r$ is just the cosine of the incident arrival ray direction with respect to the normal to the recording surface at $\mathbf{x}_r$, and $\hat{\mathbf{a}}_r \cdot \mathbf{u}^{P}$ is the recorded vertical component u_z^{P}. Substituting (35), (16) and (41) into (39) we obtain:

$$\hat{\mathbf{a}}_r \cdot \mathbf{u}^{P}(\mathbf{x}_r) = -\int_{\mathcal{V}} \frac{i\omega}{\alpha^2} A_s A_r e^{i\omega\tau_{sr}} \left\{ [\alpha\nabla\lambda - \lambda\nabla\alpha] \cdot \hat{\mathbf{t}}_r^{P} + 2\,[\alpha\nabla\mu - \mu\nabla\alpha] \cdot (\hat{\mathbf{t}}_s^{P}\hat{\mathbf{t}}_s^{P}) \cdot \hat{\mathbf{t}}_r^{P} \right\} d\mathcal{V} \,, \tag{44}$$

where we have compacted the notation: $\tau_{sr} = \tau_s + \tau_r$. Equation (44) defines how to forward model non-Zoeppritz, non-geometric P-P reflections and diffractions created by gradients in the material properties α, λ and μ. We note that the concept of a single "reflecting surface" is generalized to three such surfaces, each defined by $\nabla\alpha$, $\nabla\lambda$ and $\nabla\mu$, which are not necessarily identical! We also note that the scattering contribution from the parameter gradients involves no plane-wave assumption, and therefore is more general than the Zoeppritz coefficients. Finally, since $\hat{\mathbf{t}}_s^{P}$ and $\hat{\mathbf{t}}_r^{P}$ are arbitrary incident and emergent directions at the reflecting "surface", they do not satisfy Snell's Law in general, and therefore create a total scattered response which is a hybrid combination of geometric plane-wave reflection (Aki and Richards, 1980), and Rayleigh-Sommerfeld diffraction (Goodman, 1968).

Kirchhoff $\grave{P}\acute{P}$ body force equivalent

In this section, we now seek to distinguish the geometric (specular) reflection contributions from the diffraction contributions to the total scattered response derived in (44). Without loss of generality, we define a local geometric/specular/Snell reflection wavefield $\mathbf{u}^{PP}$ such that

$$\mathbf{u}^{PP}(\mathbf{x};\mathbf{x}_s) = [\mathbf{u}^{P}(\mathbf{x};\mathbf{x}_s) \cdot \hat{\mathbf{t}}^{P}(\mathbf{x};\mathbf{x}_s)] \;\; \grave{P}\acute{P}(\mathbf{x};\mathbf{x}_s) \;\; \hat{\mathbf{t}}^{PP}(\mathbf{x};\mathbf{x}_s) \,. \tag{45}$$

The term $\grave{P}\acute{P}$ is a geometric reflection coefficient, which may or may not be related to the Zoeppritz plane-wave coefficient, as discussed later. The unit vector $\hat{\mathbf{t}}^{PP}$ is the direction of geometric reflection given by satisfying Snell's Law at the reflecting surface, as sketched in Figure **??**:

$$\hat{\mathbf{t}}^{PP} = \hat{\mathbf{t}}^{P} \cdot (\mathbf{I} - 2\hat{\mathbf{n}}\hat{\mathbf{n}}) \,, \tag{46}$$

where $\hat{\mathbf{n}}$ is the unit normal to the reflecting surface at $\mathbf{x}$. Given this definition of $\hat{\mathbf{t}}^{PP}$, the following identity also relates $\hat{\mathbf{t}}^{P}$ to $\hat{\mathbf{t}}^{PP}$:

$$\hat{\mathbf{t}}^{PP} \cdot \hat{\mathbf{n}} = -\hat{\mathbf{t}}^{P} \cdot \hat{\mathbf{n}} \,. \tag{47}$$

We derive the following useful properties for $\mathbf{u}^{PP}$:

$$\nabla \cdot \mathbf{u}^{PP} = \frac{i\omega}{\alpha} \hat{\mathbf{t}}^{PP} \cdot \mathbf{u}^{PP} \,, \tag{48}$$

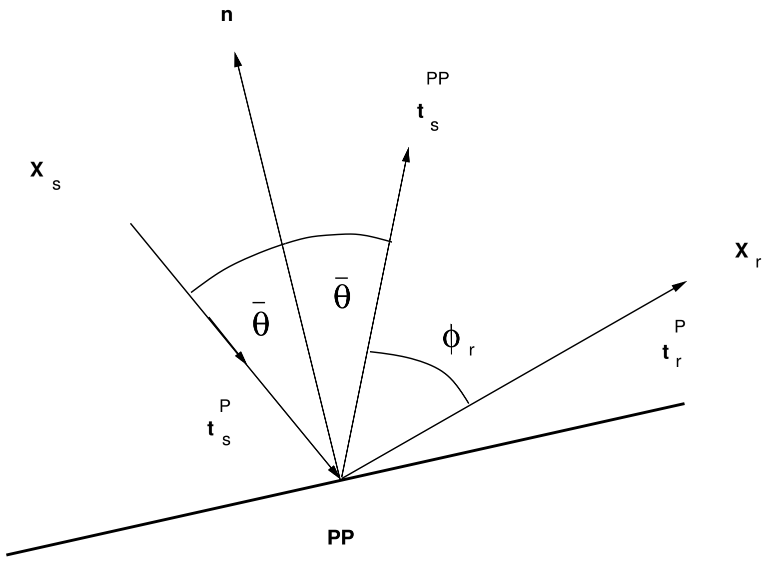

Figure 1: Scattering geometry. david1-raygeom [NR]

and

$$\nabla \mathbf{u}^{PP} = \frac{i\omega}{\alpha} \hat{\mathbf{t}}^{PP} \mathbf{u}^{PP} \ . \tag{49}$$

Then, we evaluate the stress field σ^{PP} associated with this geometric reflectivity as:

$$\sigma^{PP} = \lambda(\nabla \cdot \mathbf{u}^{PP})\mathbf{I} + 2\mu \nabla \mathbf{u}^{PP} = \frac{i\omega}{\alpha} \left[\lambda(\hat{\mathbf{t}}^{PP} \cdot \mathbf{u}^{PP})\mathbf{I} + 2\mu \hat{\mathbf{t}}^{PP} \mathbf{u}^{PP} \right] \ . \tag{50}$$

Next, we decompose the total stress gradient into background and scattered stress field gradient components, as suggested by the Born analogy and physical interpretation of (36), (37) and (38):

$$\nabla \cdot \sigma^{P} = \nabla_o \cdot \sigma^{P} + \nabla_o \cdot \sigma^{PP} \ , \tag{51}$$

where ∇_o is the gradient with respect to a smooth (reflectionless) background model, $\nabla_o \cdot \sigma^{P}$ refers to the direct stress divergence wavefield in the smooth background medium, and $\nabla_o \cdot \sigma^{PP}$ refers to the scattered (reflected) stress divergence wavefield in the smooth background model. There is an implicit and as yet unexplored relationship between the Born model (36) and our Kirchhoff model (51):

$$\nabla \cdot \sigma^{\delta m} = \nabla_o \cdot \sigma^{PP} \ . \tag{52}$$

Our Kirchhoff decomposition (51) assumes a linear relationship between the total stress divergence in the true medium versus the direct and scattered stress divergences in the smooth background medium.

We evaluate the scattered stress divergence $\nabla_o \cdot \sigma^{PP}$ as:

$$\nabla_o \cdot \sigma^{PP} = \frac{i\omega}{\alpha} \left[\lambda \nabla_o \mathbf{u}^{PP} \cdot \hat{\mathbf{t}}^{PP} + 2\mu \hat{\mathbf{t}}^{PP} \cdot \nabla_o \mathbf{u}^{PP} \right] + \mathrm{O}(\nabla_o \alpha, \nabla_o \lambda, \nabla_o \mu) \; . \tag{53}$$

The terms of order $(\nabla_o \alpha, \nabla_o \lambda, \nabla_o \mu)$ vanish because the gradient ∇_o is taken with respect to the smooth reflectionless background medium, and contains no source of scattering. Continuing to evaluate $\nabla_o \cdot \sigma^{PP}$:

$$\begin{aligned} \nabla_o \cdot \sigma^{PP} &\approx -\frac{\omega^2}{\alpha^2} \left[\lambda \hat{\mathbf{t}}^{PP} \mathbf{u}^{PP} \cdot \hat{\mathbf{t}}^{PP} + 2\mu \hat{\mathbf{t}}^{PP} \cdot \hat{\mathbf{t}}^{PP} \mathbf{u}^{PP} \right] \\ &= -\frac{\omega^2}{\alpha^2} (\lambda + 2\mu) \mathbf{u}^{PP} \\ &= -\rho \omega^2 \mathbf{u}^{PP} \; , \end{aligned} \tag{54}$$

where we have assumed that

$$\nabla_o \mathbf{u}^{PP} \approx \nabla \mathbf{u}^{PP} \; , \tag{55}$$

which implies that that *propagation* directions $\hat{\mathbf{t}}^{PP}$, traveltimes τ and spreading amplitudes A^{PP} of the scattered wavefield as it propagates from the scattering point to the observation point, are approximately the same in the smooth background as in the true background medium. The divergence of the total stress field in the true medium is then:

$$\nabla \cdot \sigma^{P} = \nabla_o \sigma^{P} + \nabla_o \sigma^{PP} = -\rho \omega^2 (\mathbf{u}^{P} - \mathbf{u}^{PP}) \; . \tag{56}$$

The body force equivalent $\mathbf{f}^{P}$ with respect to $\mathbf{u}^{PP}$ is:

$$\mathbf{f}^{P} = -\rho \omega^2 \mathbf{u}^{P} - \nabla \cdot \sigma^{P} = +\rho \omega^2 \mathbf{u}^{PP} \; . \tag{57}$$

Comparing (35) to (57) we see that

$$\mathbf{u}^{PP} = \frac{|\mathbf{u}^{P}|}{i\omega\rho\alpha^2} \left[(\alpha \nabla \lambda - \lambda \nabla \alpha) + 2(\alpha \nabla \mu - \mu \nabla \alpha) \right] \cdot \hat{\mathbf{t}}^{P} \hat{\mathbf{t}}^{P} \; , \tag{58}$$

and since

$$\hat{\mathbf{n}}\cdot\mathbf{u}^{PP} \equiv \mathbf{u}^{P}\cdot\hat{\mathbf{t}}^{P}\grave{P}\acute{P}\hat{\mathbf{t}}^{PP}\cdot\hat{\mathbf{n}} = -|\mathbf{u}^{P}|\grave{P}\acute{P}\hat{\mathbf{t}}^{P}\cdot\hat{\mathbf{n}} \ , \tag{59}$$

the volumetric body force equivalent geometric reflection coefficient $\grave{P}\acute{P}$ can be identified as

$$\grave{P}\acute{P} = \frac{-1}{i\omega\rho\alpha^2}\left[(\alpha\nabla\lambda - \lambda\nabla\alpha) + 2(\alpha\nabla\mu - \mu\nabla\alpha)\right]\cdot\hat{\mathbf{t}}^{P} \ . \tag{60}$$

Finally, we calculate the scattered field $\mathbf{u}^{P}(\mathbf{x}_r)$ in terms of the geometric reflection coefficient $\grave{P}\acute{P}$ using (39), (57), (45) and (40):

$$\hat{\mathbf{a}}_r\cdot\mathbf{u}^{P}(\mathbf{x}_r) = \int_{\mathcal{V}} \rho\omega^2 A_s A_r e^{i\omega\tau_{sr}}\grave{P}\acute{P}\ (\hat{\mathbf{t}}_s^{PP}\cdot\hat{\mathbf{t}}_r^{P})\ d\mathcal{V}(\mathbf{x}) \ . \tag{61}$$

For clarity, we define the angles shown in Figure **??**:

$$-\hat{\mathbf{t}}^{P}(\mathbf{x};\mathbf{x}_s)\cdot\hat{\mathbf{n}}(\mathbf{x}) = \cos\theta_s = \cos\bar{\theta} \ , \tag{62}$$

$$\hat{\mathbf{t}}^{P}(\mathbf{x};\mathbf{x}_r)\cdot\hat{\mathbf{n}}(\mathbf{x}) = \cos\theta_r \ , \tag{63}$$

$$\hat{\mathbf{t}}^{PP}(\mathbf{x};\mathbf{x}_s)\cdot\hat{\mathbf{t}}^{P}(\mathbf{x};\mathbf{x}_r) = \cos\phi_r = \cos(\theta_s + \theta_r - 2\bar{\theta}) \ , \tag{64}$$

and

$$-\hat{\mathbf{t}}^{P}(\mathbf{x};\mathbf{x}_s)\cdot\hat{\mathbf{t}}^{P}(\mathbf{x};\mathbf{x}_r) = \cos\theta_{sr} = \cos(\theta_s + \theta_r) \ . \tag{65}$$

With these definitions, (61) can be written in compact form as:

$$\hat{\mathbf{a}}_r\cdot\mathbf{u}^{P}(\mathbf{x}_r) = \int_{\mathcal{V}} \rho\omega^2 A_s A_r e^{i\omega\tau_{sr}}\grave{P}\acute{P}\cos\phi_r\, d\mathcal{V}(\mathbf{x}) \ . \tag{66}$$

To recap (66), the density at a subsurface point is denoted $\rho(\mathbf{x})$, and the geometric reflection coefficient at that point is $\grave{P}\acute{P}(\mathbf{x})$. The amplitude terms A_s and A_r represent the cumulative geometric spreading, transmission loss, Q-attenuation, etc., from the source and receiver to the subsurface point $\mathbf{x}$ respectively. The factor A_r also includes the vector component projection at the surface location $\mathbf{x}_r$ as defined by (42) and (43). The term τ_{sr} is the total traveltime from source at $\mathbf{x}_s$ to the subsurface point $\mathbf{x}$ and back up to the receiver at $\mathbf{x}_r$. Finally, the diffraction weight $\cos\phi_r$ represents the angle between the anticipated geometric specular reflection direction $\hat{\mathbf{t}}_s^{PP}$ and the actual diffraction direction $\hat{\mathbf{t}}_r^{P}$. In the case of specular reflection when $\hat{\mathbf{t}}_s^{PP} = \hat{\mathbf{t}}_r^{P}$, $\phi_r = 0$ and so $\cos\phi_r = 1$.

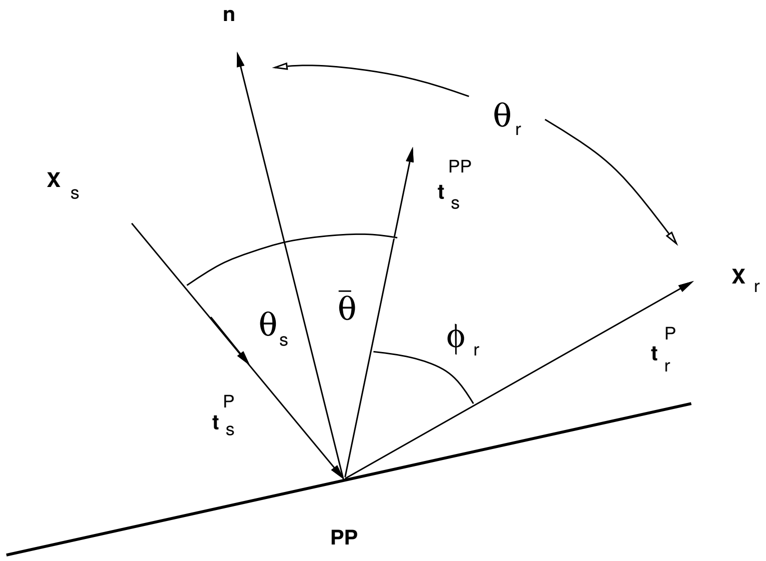

Figure 2: Generalized reflection ray and angle geometries. $\boxed{\text{david1-anglegeom}}$ [NR]

We now make some general comments about the forward modeling theory given by (66).

- $\hat{\mathbf{a}}_r \cdot \mathbf{u}^P$ is in fact $\hat{\mathbf{a}}_r \cdot \mathbf{u}^{PP}$ since we have removed the background field contribution by assuming a smooth background when solving for $\mathbf{f}^P$ in (57).
- The scattered wavefield is *linear* with respect to $\grave{P}\acute{P}$. This follows in that if the local reflector volume is subdivided into multiple smaller volumes, by linear superposition the volume integration result of (66) should not change. If the model is not ray valid for interfaces (i.e., interface topography varies faster than a spatial wavelength of the wavefield), then a linearized version of $\grave{P}\acute{P}$ with respect to material property contrasts, such as (60), is required. Otherwise, if interfaces are ray valid, then by extension a $\grave{P}\acute{P}$ coefficient which is nonlinearly related to material property contrasts may also be appropriate, such as Zoeppritz.
- $\cos\phi_r$ is symmetric with respect to θ_s and θ_r (reciprocity), but not $\grave{P}\acute{P}(\theta_s)$.
- It is important to note that the volume integration (66) models a single trace for any arbitrary source and receiver location. There is no "preferred" acquisition geometry for this synthesis; it works for shot gathers as well as random trace orientations. In particular, (66) is perfectly adequate for *constant offset* survey data, which will be the focus of the following inverse theory section.

This completes the forward modeling theory part of our paper that is necessary to proceed onward to the inverse estimation problem.

INVERSE ESTIMATION THEORY

The inverse problem

The least-squares inverse problem is formulated as follows. Consider our observations consist of a set of constant offset scalar data $D(\mathbf{x}_m; \mathbf{x}_h, \omega)$ measured along the $\hat{\mathbf{a}}_r$ receiver component direction. A constant-offset l_2 misfit energy functional can be defined as

$$E(\mathbf{x}_h) = \frac{1}{2} \int_\omega \int_{\mathbf{x}_m} \left[D(\mathbf{x}_m; \mathbf{x}_h, \omega) - U(\mathbf{x}_m; \mathbf{x}_h, \omega) \right]^2 \, d\mathbf{x}_m \, d\omega \ , \tag{67}$$

where $U = \hat{\mathbf{a}}_r \cdot \mathbf{u}^P$. The misfit error energy function (67) attempts to fit the theoretical response $\hat{\mathbf{a}}_r \cdot \mathbf{u}^P$ to the observed data D, and will give minimum error for the optimal solution of $\grave{P}\acute{P}$ and $\bar{\theta}$. Recall that from (66):

$$U(\mathbf{x}_m; \mathbf{x}_h, \omega) = \hat{\mathbf{a}}_r \cdot \mathbf{u}^P = \int_{\mathcal{V}} \rho \omega^2 A_s A_r e^{i\omega\tau_{sr}} \grave{P}\acute{P} \cos\phi_r \, d\mathcal{V}(\mathbf{x}) \ . \tag{68}$$

Since U is a function of $\grave{P}\acute{P}$ and $\bar{\theta}$, which are the quantities we want to estimate from the data D, we minimize (67) with respect to $\grave{P}\acute{P}$ and the geometric specular angle $\bar{\theta}$, which leads to two coupled normal equations:

$$\frac{\partial E}{\partial \grave{P}\acute{P}} = -\int_\omega \int_{\mathbf{x}_m} [D - U] \left[\int_V \rho \omega^2 A_s A_r \cos\phi_r e^{i\omega\tau_{sr}} dV \right] d\mathbf{x}_m \, d\omega \ , \tag{69}$$

and

$$\frac{\partial E}{\partial \bar{\theta}} = -2 \int_\omega \int_{\mathbf{x}_m} [D - U] \left[\int_V \rho \omega^2 A_s A_r \grave{P}\acute{P} \sin\phi_r e^{i\omega\tau_{sr}} dV \right] d\mathbf{x}_m \, d\omega \ . \tag{70}$$

In general, these two coupled equations should be solved simultaneously for $\grave{P}\acute{P}$ and $\bar{\theta}$. As that is rather complicated, we now present a much simpler approximate approach. The equations can be *decoupled* by the stationary phase (high-frequency) approximation, in which the major contribution to (68) occurs near the specular point when $\phi_r \approx 0$. In this case, the $\grave{P}\acute{P}$ equation can be solved independently of $\bar{\theta}$, and the result can be backsubstituted into the original normal equation for $\bar{\theta}$. It is important to note that by assuming the *generalized* form of diffraction-reflection in (66), we have derived *two* equations, one for each of $\grave{P}\acute{P}$ and $\bar{\theta}$. Now we will proceed to solve only the $\grave{P}\acute{P}$ equation under stationary phase, and use the $\grave{P}\acute{P}$ result to solve the $\bar{\theta}$ equation. Had we *started* with the assumption of specular reflection (stationary phase), we would have had only one equation for *specular* $\grave{P}\acute{P}$, and *no* equation describing $\bar{\theta}$! That is a very important distinction.

The first step in the decoupling is to apply the method of stationary phase to the volume integral within the misfit error functional E of (67). The phase component γ of the volume integral is

$$\gamma(\mathbf{x};\mathbf{x}_s,\mathbf{x}_r) = \omega\tau_{sr}(\mathbf{x};\mathbf{x}_s,\mathbf{x}_r) = \omega\left[\tau_s(\mathbf{x};\mathbf{x}_s) + \tau_r(\mathbf{x};\mathbf{x}_r)\right] \ . \tag{71}$$

The stationary point of the phase with respect to the integration variable $\mathbf{x}$ is defined by the equation:

$$\nabla\gamma = \omega\nabla\tau_{sr} = \omega(\nabla\tau_s + \nabla\tau_r) = 0 \ . \tag{72}$$

In particular,

$$\nabla\tau_s(\mathbf{x})\cdot\hat{\mathbf{n}}(\mathbf{x}) = -\nabla\tau_r(\mathbf{x})\cdot\hat{\mathbf{n}}(\mathbf{x}) \ , \tag{73}$$

where $\hat{\mathbf{n}}$ is the normal to the reflecting surface at the point $\mathbf{x}$. Since $\nabla\tau = \hat{\mathbf{t}}^P/\alpha$ as in (20), the stationary condition (73) is equivalent to:

$$\cos\theta_s(\mathbf{x}) = \cos\theta_r(\mathbf{x}) \ , \tag{74}$$

which in turn is simply stating the law of specular reflection for a $\grave{P}\acute{P}$ wave at a reflecting boundary. In other words, the stationary point, and hence the major contribution to the integral of the misfit error functional, occurs at the condition of specular reflection, when $\phi_r \approx 0$. In this case, the misfit error at stationarity reduces to:

$$E(\mathbf{x}_h) \approx \frac{1}{2}\int_\omega\int_{\mathbf{x}_m}\left[D(\mathbf{x}_m;\mathbf{x}_h,\omega) - \int_V \rho\omega^2 A_s A_r \grave{P}\acute{P} e^{i\omega\tau_{sr}}\, dV\right]^2 d\mathbf{x}_m\, d\omega \ . \tag{75}$$

Now the error misfit functional (75) is in standard linear form, and can be solved for $\grave{P}\acute{P}$ with a traditional Gauss-Newton gradient optimization method. The solution for $\grave{P}\acute{P}$ should then be backsubstituted into the $\bar{\theta}$ normal equation, and this decoupling should lead to an l_2 solution for $\bar{\theta}$, which would not have been otherwise possible had we *started* directly with the specular form (75).

Reflectivity estimation

Under the stationary phase approximation, the $\grave{P}\acute{P}$ equation is in the standard linear form:

$$\mathbf{d} = \mathbf{F}\mathbf{m} \ , \tag{76}$$

where $\mathbf{m} = \grave{P}\acute{P}$, $\mathbf{d} = D$, and F is the forward theoretical mapping of $\grave{P}\acute{P}$ to U, given (66). This linear form has a well-known damped least-squares Gauss-Newton solution (e.g., Gill et al., 1981):

$$\mathbf{m} \approx -\mathbf{H}^{-1}\mathbf{g} \approx (\mathbf{F}'\mathbf{F} + \epsilon^2)^{-1}\mathbf{F}'\mathbf{d} \ , \tag{77}$$

where $\mathbf{g}$ and $\mathbf{H}$ are the gradient and Hessian of E respectively, and $\mathbf{F}'$ is the adjoint operator to $\mathbf{F}$. The adjoint operator is *defined* by the inner product:

$$< \mathbf{d}, \mathbf{Fm} > = < \mathbf{F}'\mathbf{d}, \mathbf{m} > \ . \tag{78}$$

Writing down the integral equation implied in (78), interchanging the order of integration, and taking the complex conjugate, results in an integral expression for the adjoint operator:

$$\mathbf{F}'\{\cdot\} = \int_\omega \int_{\mathbf{x}_m} \rho\omega^2 A_s A_r \{\cdot\} e^{-i\omega\tau_{sr}} \, d\mathbf{x}_m \, d\omega \ . \tag{79}$$

In this case, the gradient can be derived as

$$\mathbf{g}(\mathbf{x}; \mathbf{x}_h) = -\mathbf{F}'\mathbf{d} = -\int_\omega \int_{\mathbf{x}_m} \rho\omega^2 A_s A_r D e^{-i\omega\tau_{sr}} \, d\mathbf{x}_m \, d\omega \ . \tag{80}$$

Neglecting second-derivative terms, the Hessian can be derived in the Gauss-Newton sense as:

$$\mathbf{H}(\mathbf{x}, \mathbf{x}^{'}; \mathbf{x}_h) = \mathbf{F}'\mathbf{F}\{\cdot\} = \int_\omega \int_{\mathbf{x}_m} \rho\omega^2 A_s A_r \left[\int_{V'} \rho'\omega^2 A_s' A_r' \{\cdot\} e^{i\omega\tau_{sr}'} \, dV' \right] e^{-i\omega\tau_{sr}} \, d\mathbf{x}_m \, d\omega \ . \tag{81}$$

Evaluation of one "column" of the Hessian operator requires a complete forward modeling response to an impulse located at a *single* subsurface location $\mathbf{x}^{'}$, followed by a complete prestack depth migration of that impulse response back to *all* subsurface positions $\mathbf{x}$. Therefore, the complete evaluation of the full Hessian operator requires $N_{\mathbf{x}}$ forward modeling runs plus $N_{\mathbf{x}}$ prestack depth migrations, where $N_{\mathbf{x}}$ is the total number of discrete surface points under consideration. This would be extremely expensive, if not impossible to compute!

In this form, the Hessian is spatially non-diagonal in the sense that it tries to incorporate and compensate for all point-to-point correlations of reflectivity in the subsurface, at $\mathbf{x}$ due to $\mathbf{x}^{'}$. This non-diagonality should not be confused with *multi-parameter* crosscorrelations which occur in the case of acoustic or elastic parameter inversions (e.g., Beydoun and Mendes, 1989). There is only a single parameter being estimated here ($\grave{P}\acute{P}$), and it is likely to be spatially correlated due to finite data bandwidth. The Hessian $\mathbf{H}$ in (81) is trying to *deconvolve* that spatial correlation. The effect of applying the full Hessian is to perform a *least-squares acquisition geometry and aperture compensation* to the reflectivity estimate.

In the interest of efficiency, the Hessian operator can be diagonalized (i.e., ignoring spatial correlations of $\grave{P}\acute{P}$), by assuming the "·" in the volume integrand of (81) is a spatially uncorrelated delta function $\delta(\mathbf{x}^{'} - \mathbf{x})$ (e.g., Le Bras and Clayton, 1988). In this case, we find a diagonal operator $\mathbf{h}(\mathbf{x}, \mathbf{x}^{'}; \mathbf{x}_h)$ which is the diagonalized Hessian such that:

$$\mathbf{h}(\mathbf{x}, \mathbf{x}^{'}; \mathbf{x}_h) \approx \mathbf{H}(\mathbf{x}, \mathbf{x}^{'}; \mathbf{x}_h) \ , \tag{82}$$

where the elements along the diagonal are given by:

$$\mathbf{h}(\mathbf{x} = \mathbf{x}^{'}; \mathbf{x}_h) = \mathbf{H}(\mathbf{x} = \mathbf{x}^{'}; \mathbf{x}_h) = \mathrm{Diag}\{\mathbf{F}'\mathbf{F}\} = \int_\omega \int_{\mathbf{x}_m} \rho^2 \omega^4 A_s^2 A_r^2 \, d\mathbf{x}_m \, d\omega + \epsilon^2(\mathbf{x}; \mathbf{x}_h) \ , \tag{83}$$

where the ϵ^2 term has been added for stability. The inverse diagonal Hessian is then simply the inverse of each diagonal element of $\mathbf{h}(\mathbf{x}, \mathbf{x}^{'})$:

$$\mathbf{H}^{-1}(\mathbf{x}, \mathbf{x}^{'}; \mathbf{x}_h) \approx \mathbf{h}^{-1}(\mathbf{x}, \mathbf{x}^{'}; \mathbf{x}_h) \ , \tag{84}$$

where $\mathbf{h}^{-1}$ is another diagonal operator with elements:

$$\mathrm{Diag}\{\mathbf{h}^{-1}\} = \left(\int_\omega \int_{\mathbf{x}_m} \rho^2 \omega^4 A_s^2 A_r^2 \, d\mathbf{x}_m \, d\omega + \epsilon^2(\mathbf{x}; \mathbf{x}_h) \right)^{-1} \ . \tag{85}$$

Applying the approximate inverse diagonal Hessian operator (85) to the gradient (80) results in an approximate l_2 solution for the $\grave{P}\acute{P}$ geometric reflection coefficient:

$$\grave{P}\acute{P}(\mathbf{x}; \mathbf{x}_h) = -\mathbf{H}^{-1}\mathbf{g} \approx -\mathbf{h}^{-1}\mathbf{g} = \frac{\int_\omega \int_{\mathbf{x}_m} \rho \omega^2 A_s A_r D e^{-i\omega\tau_{sr}} \, d\mathbf{x}_m \, d\omega}{\int_\omega \int_{\mathbf{x}_m} \rho^2 \omega^4 A_s^2 A_r^2 \, d\mathbf{x}_m \, d\omega + \epsilon^2(\mathbf{x}; \mathbf{x}_h)} \ . \tag{86}$$

The approximate diagonal Hessian solution (86) costs little more than a single conventional prestack migration in terms of floating point operations. However, one drawback is that it requires twice the memory, since the $\mathbf{g}$ and $\mathbf{h}$ images must be stored separately during the estimation (migration) process. They may only be combined as in (86) after both have been completely imaged. This seems to be a small price to pay for a reasonably good l_2 $\grave{P}\acute{P}(\bar{\theta})$ amplitude estimate.

It should be noted that the form and weight structure of the l_2 inverse solution (86) is somewhat similar, but different in detail, to the trial solution of Bleistein (1987). In particular, (86) involves two separate but simultaneous images to be evaluated, the gradient (numerator) being a weighted Kirchhoff prestack depth migration, and the approximate inverse Hessian (denominator) being an accumulation of the squared migration weights. Bleistein's solution involves only one migration integral since it is not a least-squares estimate, and his different migration kernel amplitude weights will give a different $\grave{P}\acute{P}(\bar{\theta})$ amplitude result in general.

Reflection angle estimation

In principle, an l_2 solution for the reflection angles $\bar{\theta}$ can be estimated directly from the reflection data D by substituting the solution (86) into the normal equation $\partial E/\partial\bar{\theta} = 0$. A difficulty arises from the fact that the kernel functions of (70) are *nonlinearly* related to $\bar{\theta}$ by the cosine. In this case,

$$\mathbf{Fm} \rightarrow \mathbf{F}\{\bar{\theta}\} = \int_{\mathcal{V}} \rho\omega^2 A_s A_r e^{i\omega\tau_{sr}} \grave{P}\acute{P} \cos(\theta_{sr} - 2\bar{\theta})\, d\mathcal{V} \ , \tag{87}$$

is a nonlinear forward mapping between the model $\mathbf{m} = \bar{\theta}$ and the data U.

We solve this nonlinear inverse problem for $\bar{\theta}$ by *linearizing* (87) with respect to a new model parameter: $\mathbf{m} = \cos 2\bar{\theta}$. Using the standard cosine expansion,

$$\cos\phi_r \equiv \cos(\theta_{sr} - 2\bar{\theta}) = \cos\theta_{sr}\cos 2\bar{\theta} + \sin\theta_{sr}\sin 2\bar{\theta} \ . \tag{88}$$

and using the small angle approximation:

$$\theta_{sr}\, , 2\bar{\theta} \ll \pi/4 \ , \tag{89}$$

we approximate $\cos\phi_r$ as:

$$\cos\phi_r \approx \cos\theta_{sr}\cos 2\bar{\theta} \ . \tag{90}$$

We note that under this approximation, at the specular reflection (stationary point):

$$\cos\phi_r = 1 \approx \cos\theta_{sr}\cos 2\bar{\theta} \ . \tag{91}$$

We will use this relation (91) later to "undo" the small angle approximation after we obtain a linearized solution, as will be discussed later.

Now, under approximation (90), we obtain a linearized forward theory relating the new model parameter $\mathbf{m} = \cos 2\bar{\theta}$ to the data U:

$$\mathbf{Fm} = \mathbf{F}\{\cos 2\bar{\theta}\} = \int_{\mathcal{V}} \rho\omega^2 A_s A_r e^{i\omega\tau_{sr}} \grave{P}\acute{P} \cos\theta_{sr}\cos 2\bar{\theta}\, d\mathcal{V} \ . \tag{92}$$

This linearized map is now in standard linear form and can be solved with an analogous Gauss-Newton gradient method as for the case of the $\grave{P}\acute{P}$ inverse problem. We derive the new gradient operator $\mathbf{g}_2$ as:

$$\mathbf{g}_2(\mathbf{x};\mathbf{x}_h) = -\mathbf{F}'\mathbf{d} = -\int_\omega \int_{\mathbf{x}_m} \rho\omega^2 A_s A_r e^{-i\omega\tau_{sr}} \grave{P}\acute{P} \cos\theta_{sr} D \, d\mathbf{x}_m \, d\omega \ . \tag{93}$$

Neglecting second-derivative terms, the Hessian can be evaluated in the classic Gauss-Newton sense as:

$$\mathbf{H}_2 = \mathbf{F}'\mathbf{F} + \epsilon^2 = \int_\omega \int_{\mathbf{x}_m} \rho\omega^2 A_s A_r e^{-i\omega\tau_{sr}} \grave{P}\acute{P} \cos\theta_{sr} \left[\int_{V'} I_1(\mathbf{x}') \ dV' \right] d\mathbf{x}_m \, d\omega + \epsilon^2(\mathbf{x};\mathbf{x}_h) \ , \tag{94}$$

where

$$I_1 = \rho'\omega^2 A'_s A'_r e^{i\omega\tau'_{sr}} \grave{P}\acute{P} \cos\theta'_{sr} \{\cdot\} \ . \tag{95}$$

At this point, $\cos 2\bar{\theta}$ could be estimated as $\mathbf{m} \approx -\mathbf{H}_2^{-1}\mathbf{g}_2$ using the gradient and Hessian expressions (93) and (94), and substituting the results of a previous estimation of $\grave{P}\acute{P}$ from (86). However, this would be very inefficient for two reasons: (1) the full Hessian of equation (94) requires $N_{\mathbf{x}}$ forward modeling and migration steps, and (2) the values of $\grave{P}\acute{P}$ required by expressions (93) and (94) would need to be calculated by a prior prestack depth migration given by (86). For this reason, we now show how to approximate $\grave{P}\acute{P}$ and diagonalize $\mathbf{H}_2$ in (93) and (94), so that a complete estimate of $\grave{P}\acute{P}(\bar{\theta})$ can be made for the same cost as one single prestack depth migration.

First we diagonalize the Hessian operator (94), by evaluating the $\mathcal{V}'$ integral in (94) at the stationary point where:

$$\int_{V'} \rho'\omega^2 A'_s A'_r e^{i\omega\tau'_{sr}} \grave{P}\acute{P} \cos\theta_{sr} \{\cdot\} \, dV' \to \rho\omega^2 A_s A_r \grave{P}\acute{P} \cos 2\bar{\theta} \ , \tag{96}$$

Now we try to "undo" the small angle approximation (90) by noting that at the point of stationary phase, which gives the most contribution to $\mathbf{g}_2$ and $\mathbf{H}_2$, that

$$\cos\theta_{sr} \cos 2\bar{\theta} \to 1 \ , \tag{97}$$

as expressed in (91).

With these simplifying assumptions (96) and (97), the diagonal Hessian becomes:

$$\mathbf{H}_2 = \mathbf{F}'\mathbf{F} + \epsilon^2 \approx \mathbf{h}_2 \ , \tag{98}$$

where the diagonal elements are given as

$$\text{Diag}\{\mathbf{H}_2\} = \text{Diag}\{\mathbf{h}_2\} = \int_\omega \int_{\mathbf{x}_m} \rho^2 \omega^4 A_s^2 A_r^2 (\grave{P}\acute{P})^2 e^{-i\omega\tau_{sr}}\, d\mathbf{x}_m\, d\omega + \epsilon^2(\mathbf{x};\mathbf{x}_h)\ . \quad (99)$$

Also, we want to avoid computing a first prestack depth migration for $\grave{P}\acute{P}$ to serve as input for a second prestack depth migration estimate of $\cos 2\bar{\theta}$, although one could certainly do this if computer time was not an issue. To economize, we assume a stationary specular reflection coefficient value for $\grave{P}\acute{P}$, given from the data as:

$$\grave{P}\acute{P} \rightarrow \frac{D}{\rho\omega^2 A_s A_r}\ , \quad (100)$$

since at the stationary point, (87) reduces to:

$$D' \rightarrow \rho' \omega^2 A_s' A_r' \grave{P}\acute{P}'\ . \quad (101)$$

Substituting (100) into (93) and (99), we obtain a very efficient estimation solution for the specular reflection angle $\bar{\theta}$ directly from the recorded data D:

$$\cos 2\bar{\theta}(\mathbf{x};\mathbf{x}_h) = -\mathbf{H}_2^{-1}\mathbf{g}_2 \approx -\mathbf{h}_2^{-1}\mathbf{g}_2 = \frac{\int_\omega \int_{\mathbf{x}_m} D^2 e^{-i\omega\tau_{sr}} \cos\theta_{sr}\, d\mathbf{x}_m\, d\omega}{\int_\omega \int_{\mathbf{x}_m} D^2 e^{-i\omega\tau_{sr}}\, d\mathbf{x}_m\, d\omega + \epsilon^2(\mathbf{x};\mathbf{x}_h)}\ . \quad (102)$$

Equation (102) is the (implicit) least-squares estimate of $\bar{\theta}$ which we seek.

We now discuss the physical interpretation of (102) to lend insight. Consider a fixed point $\mathbf{x}$ in the subsurface. As we migrate a constant offset section into $\mathbf{x}$, the angle θ_{sr} between the source and receiver rays ranges from $\theta_{sr} \approx 0$ at $\mathbf{x}_m = \mathbf{x}_{min}$, to $\theta_{sr} \approx 2\bar{\theta}$ near the specular midpoint, and back to $\theta_{sr} \approx 0$ at $\mathbf{x}_m = \mathbf{x}_{max}$. Analogously, the diffraction-reflection coefficient $R_{PP} = \grave{P}\acute{P} \cos\phi_r$ varies from $R_{PP} \approx 0$ (pure diffraction) to $R_{PP} \approx \grave{P}\acute{P}(\bar{\theta})$ (specular reflection), to $R_{PP} \approx 0$ (pure diffraction) again, over the same midpoint integration range. Hence, it is apparent that R_{PP} will attain a maximal peak amplitude at the specular midpoint, whereupon $R_{PP} = \grave{P}\acute{P}(\bar{\theta})$ and $\theta_{sr} = 2\bar{\theta}$. Hence, (102) represents a weighted first moment average of the data (squared), which has a central amplitude peak at the midpoint and angle of specular reflection.

It should be noted that the estimate (102) is similar to the result of Bleistein (1987). However, our result contains different WKBJ migration weights, and is a combination of a gradient migration and a normalizing Hessian migration image. Furthermore, our solution is basically two weighted stacks of squared data values, which adds a major robustness advantage, especially at subsurface points $\mathbf{x}$ where

$|\grave{P}\acute{P}|$ tends to be small or zero, where Bleistein's result would tend toward zero division.

As an aside, given that (102) was derived from least-squares optimization theory and involves two sums of squared data values, by analogy we can conjecture that an l_1 estimate of $\bar{\theta}$ would be approximated by:

$$l_1 : \quad \cos 2\bar{\theta}(\mathbf{x};\mathbf{x}_h) \rightarrow \frac{\int_\omega \int_{\mathbf{x}_m} |D| e^{-i\omega\tau_{sr}} \cos\theta_{sr}\, d\mathbf{x}_m\, d\omega}{\int_\omega \int_{\mathbf{x}_m} |D| e^{-i\omega\tau_{sr}}\, d\mathbf{x}_m\, d\omega + \epsilon^2(\mathbf{x};\mathbf{x}_h)} \ . \tag{103}$$

It is likely that the l_1 angle estimate (103) is even more robust and less sensitive to data outliers than the l_2 result of (102). The relative merits of the l_1 versus the l_2 norm with applications to some seismic problems is discussed by Claerbout and Muir (1973).

The complete $\grave{P}\acute{P}(\bar{\theta})$ estimate

To complete the final estimation of $\grave{P}\acute{P}(\bar{\theta})$, we make a simple set of mappings from the least-squares (or l_1) estimates derived in the previous sections. A map of $\bar{\theta}(\mathbf{x};\mathbf{x}_h)$ can be obtained directly from the result of (102) or (103):

$$\mathcal{M}_1 \quad : \quad \cos\ 2\bar{\theta}(\mathbf{x};\mathbf{x}_h) \rightarrow \bar{\theta}(\mathbf{x};\mathbf{x}_h) \ . \tag{104}$$

Then, since there is a one-to-one mapping of $\bar{\theta}$ to any point $(\mathbf{x};\mathbf{x}_h)$, and $\grave{P}\acute{P}$ to the same point $(\mathbf{x};\mathbf{x}_h)$, there is a unique map of $\grave{P}\acute{P}(\mathbf{x};\mathbf{x}_h)$ and $\bar{\theta}(\mathbf{x};\mathbf{x}_h)$ to $\grave{P}\acute{P}(\bar{\theta}(\mathbf{x}))$ such that:

$$\mathcal{M}_2 \quad : \quad \{\grave{P}\acute{P}(\mathbf{x};\mathbf{x}_h), \bar{\theta}(\mathbf{x};\mathbf{x}_h)\} \rightarrow \grave{P}\acute{P}(\bar{\theta}(\mathbf{x})) \ , \tag{105}$$

which is the desired result. This completes the angle-dependent reflectivity estimation process.

CONCLUSIONS

We have derived a new Kirchhoff forward and inverse theory for modeling and estimating P-P angle-dependent reflectivity. We replaced conventional reflecting surface excitations by *equivalent body force* volumetric excitations, and then linearized the divergence of the elastic stress tensor wavefield with respect to smooth background material properties. The reflected wavefield is calculated by a volume integral over the equivalent body force distribution, and represents a hybrid combination of Zoeppritz plane-wave reflection and Rayleigh-Sommerfeld elastic diffraction.

We have posed the inverse problem as a least-squares optimization to estimate angle-dependent reflectivity, including the reflection angles, by minimizing the squared error between our forward theory and the observed seismograms. The resulting coupled normal equations are decoupled by the method of stationary phase, and then the uncoupled equations are solved by a classical Gauss-Newton gradient method with an approximate diagonal Hessian operator. The estimation for angle-dependent reflectivity requires a simultaneous calculation of four differently weighted Kirchhoff prestack depth migration images, which combine to compensate for limited acquisition aperture and enhanced reflection amplitude recovery.

ACKNOWLEDGMENTS

Part of this work was done while WBB was on a two week research visit to SEP in July 1993. We thank Jon Claerbout and Elf GRC for sponsoring WBB's visit and providing an arrangement in which to make this possible. We thank Dave Nichols for some productive discussion regarding Hessian operators and their diagonalization. Dave Nichols and Thorbjorn Rekdal provided careful reviews of the paper.

REFERENCES

Aki, K., and Richards, P. G., 1980, Quantitative seismology: W. H. Freeman and Company.

Ben-Menahem, A., and Singh, S. J., 1981, Seismic waves and sources: Springer-Verlag.

Beydoun, W. B., and Mendes, M., 1989, Elastic ray-Born l-2 migration/inversion: Geophys. J., **97**, 151–160.

Beylkin, G., 1985, Imaging of discontinuities in the inverse scattering problem by inversion of a causal generalized Radon transform: J. Math. Phys., **26**, 99–108.

Bleistein, N., 1987, On the imaging of reflectors in the earth: Geophysics, **52**, 931–942.

Červený, V., Molotkov, I. A., and Pšenčík, I., 1977, Ray method in seismology: Univerzita Karlova, Praha.

Claerbout, J. F., and Muir, F., 1973, Robust modeling with erratic data: Geophysics, **38**, 826–844.

Cunha Filho, C., 1992, Elastic modeling and migration in earth models: Ph.D. thesis, Stanford University.

de Bruin, C., 1992, Linear AVO inversion by prestack depth migration: Ph.D. thesis, Delft University, The Netherlands.

Frazer, L. N., and Sen, M. K., 1985, Kirchhoff-Helmholtz reflection seismograms in a laterally inhomogeneous multi-layered elastic medium – I. Theory: Geophys. J. R. Astr. Soc., **80**, 121–147.

Gill, P. E., Murray, W., and Wright, M. H., 1981, Practical optimization: Academic Press, Inc.

Goodman, J. W., 1968, Introduction to Fourier optics: McGraw-Hill.

Le Bras, R., and Clayton, R. W., 1988, An iterative inversion of back-scattered acoustic waves: Geophysics, **53**, 501–508.

Lumley, D. E., and Beydoun, W. B., 1991, Elastic parameter estimation by Kirchhoff prestack depth migration/inversion: Stanford Exploration Project Report, **70**, Stanford University, 165–192.

Stolt, R. H., and Weglein, A. B., 1985, Migration and inversion of seismic data: Geophysics, **50**, 2458–2472.